

TTK-11-31

RECAPP-HRI-2011-005

Constraints on axino warm dark matter from X-ray observation at the Chandra telescope and SPI

Paramita Dey*

*Institut für Theoretische Teilchenphysik und Kosmologie,
RWTH Aachen, D-52056 Aachen, Germany*

Biswarup Mukhopadhyaya†

*Regional Centre for Accelerator-based Particle Physics,
Harish-Chandra Research Institute, Chhatnag Road, Jhusi, Allahabad 211019, India*

Sourov Roy‡

*Department of Theoretical Physics, Indian Association for the Cultivation of Science,
2A & 2B Raja S.C. Mullick Road, Kolkata 700032, India*

Sudhir K. Vempati§

Centre for High Energy Physics, Indian Institute of Science, Bangalore 560012, India

(Dated: October 23, 2018)

Abstract

A sufficiently long lived warm dark matter could be a source of X-rays observed by satellite based X-ray telescopes. We consider axinos and gravitinos with masses between 1 keV and 100 keV in supersymmetric models with small R-parity violation. We show that axino dark matter receives significant constraints from X-ray observations of Chandra and SPI, especially for the lower end of the allowed range of the axino decay constant f_a , while the gravitino dark matter remains unconstrained.

PACS numbers: 11.30.Pb, 11.30.Qc, 12.60.Jv, 14.80.Va

*Electronic address: paramita@physik.rwth-aachen.de

[†]Electronic address: biswarup@hri.res.in

[‡]Electronic address: tpsr@iacs.res.in

[§]Electronic address: vempati@cts.iisc.ernet.in

I. INTRODUCTION

Though many popular supersymmetric (SUSY) models tout the lightest neutralino as the dark matter candidate, the axino or the gravitino, too, may qualify for a similar role. The stability of these dark matter candidates is generally ensured by the conservation of R -parity, defined by $R = (-1)^{(3B+L+2S)}$, where B , L and S are baryon number, lepton number and spin respectively. R -parity keeps the proton from decaying. As a by-product, it keeps the lightest supersymmetric particle (LSP) stable.

This, however, need not always be the case. It is sufficient for the dark matter particle to be stable on cosmological scales rather than be fundamentally stable. Thus a slowly decaying light axino or gravitino in an R -parity violating theory is not incompatible with a universe containing dark matter. Such a situation has a distinct phenomenology of its own.

Since the simultaneous violation of B and L would lead to unacceptably fast proton decay, one usually assumes only one of them to be violated by odd units. L -violation, in particular, leads to useful mechanisms for the generation of neutrino Majorana masses at both the tree- and one-loop levels.

Prima facie, L -violation by odd units renders the LSP unstable. This rules out the candidature of the lightest neutralino as a dark matter constituent as it tends to decay fast compared to the cosmological scales. On the other hand, if the LSP is a light gravitino or an axino, it is still possible to have a viable dark matter candidate. The requirement is that the decay of the gravitino or the axino through R -parity violating couplings should be sufficiently suppressed such that their lifetime is larger than the age of the universe. In this note, we explore this possibility and study the consequent astrophysical observations, in terms of X-rays coming from galaxies and galaxy-clusters.

The axion field in a supersymmetric model is the pseudoscalar part of an electrically neutral chiral supermultiplet Φ_a . Φ_a can be expanded as $\Phi_a = (s + ia)/\sqrt{2} + \theta\tilde{a} + \theta\theta F$, where the scalar field is denoted by s , the axion, or the pseudoscalar field, by a and their fermionic partner, the axino, is denoted by \tilde{a} . As long as SUSY is unbroken, the supermultiplet remains light, since it is protected by the Peccei-Quinn symmetry $U(1)_{\text{PQ}}$ [1–3]. The masses split, lifting the axino from the almost massless axion, if SUSY is broken. This is achieved either at the tree level or via loop diagrams. The precise value of the axino mass depends on the model. While one would typically expect the axino mass to be around M_{SUSY} , the

soft SUSY breaking scale, it has been realised [1, 2, 4] that it can be much smaller than M_{SUSY} depending on the mechanism of mass generation. In the present work, we set the axino mass as a free parameter, which could span many classes of models.

It is interesting to note that the axino is a good dark matter candidate even if R-parity is not exactly conserved. The lifetime of the axino can be very long because of the suppression from a large Peccei-Quinn (PQ) symmetry breaking scale and a small amount of R-parity violation. Axino cold dark matter (CDM) with R-parity breaking has been considered in [5] and subsequently in the context of the INTEGRAL anomaly in [6]. For non-thermal production, the axinos with a mass in the range 2–100 keV can be the warm dark matter (WDM) [7, 8].

Another candidate for warm dark matter in supersymmetric theories is the gravitino. Although the mass of the gravitino in the simple types of supergravity (mSUGRA) models is in the electroweak/TeV scale, situations with a very light gravitino, too, are often envisioned in supersymmetry. For example, light gravitinos are natural in models with gauge mediated supersymmetry breaking. Such a light gravitino can be the dark matter candidate under certain circumstances [9]. These light gravitinos can lead to novel signatures [9, 10] at colliders and accelerators and further have strong astrophysical and cosmological implications [9].

The light LSP's we are considering *i.e.* the gravitino/axino could form either cold dark matter or warm dark matter depending on their mass ranges. Typically a $\sim\text{GeV}$ dark matter would be a CDM whereas a keV dark matter would be a WDM. The exact limits however depend on the details of the candidate, its couplings etc. An axino with masses between 2 keV to 100 keV has been shown to be consistent as a warm dark matter candidate satisfying the relic density constraints [7]. In the present work we will consider this mass range for the axino, however, with R-parity violation.

A particularly simple and minimal model of R-parity violation is the case where there are *only* bilinear $\Delta L = 1$ terms in the superpotential,

$$W_{\cancel{L}} = \epsilon_i L_i H_u, \tag{1}$$

where L_i and H_u are the leptonic and up-type Higgs super-fields and the index $i = \{1, 2, 3\}$ runs over the generations. The model which has been studied over the years from many angles [11] is specified by six additional parameters at the weak scale: the three sneutrino

vacuum expectation values (VEV) and three bilinear R-parity violating couplings. The presence of these bilinear terms leads the axino to decay into a photon and a neutrino with the width given as [7]:

$$\Gamma(\tilde{a} \rightarrow \gamma \nu_i) = \frac{1}{128\pi^3} |U_{\tilde{\gamma}\tilde{Z}}|^2 \frac{m_{\tilde{a}}^3}{f_a^2} C_{a\gamma\gamma}^2 \alpha_{em}^2 \xi_i^2, \quad (2)$$

where $\xi_i = \langle \tilde{\nu}_i \rangle / v$ with the Higgs VEV given by $v = 174$ GeV,

$$U_{\tilde{\gamma}\tilde{Z}} = M_Z \sum_{\alpha} \frac{N_{\tilde{Z}\alpha} N_{\tilde{\gamma}\alpha}^*}{m_{\tilde{\chi}_\alpha}} \quad (3)$$

is the photino-zino mixing parameter containing the neutralino mixing matrix N and the mass eigenvalues $m_{\tilde{\chi}_\alpha}$, α_{em} is the fine structure constant, M_Z is the mass of the Z-boson, $m_{\tilde{a}}$ is the axino mass, f_a is the Peccei-Quinn symmetry breaking scale (up to a domain wall number), also identified with the axion decay constant, and $C_{a\gamma\gamma}$ is axion-photon-photon coupling, a model dependent quantity (See Kim [12] for a table of values). If we restrict ourselves to hadronic axion models, the axino decay into a photon and a neutrino arises from the anomaly coupling with the photon vector multiplet and the neutralino-neutrino mixing generated by the sneutrino VEV $\langle \tilde{\nu}_i \rangle$ [7].

For a suitably small mixing parameter, it is remarkable that the lifetime of the axino can exceed that of the age of the universe, for a Peccei-Quinn symmetry breaking scale of $\mathcal{O}(10^{11})$ GeV and an axino mass of 5 keV. This can be seen from the life time expression for the axino given as:

$$\tau(\tilde{a} \rightarrow \gamma \nu_i) = 3 \times 10^{35} s \left(\frac{\xi_i |U_{\tilde{\gamma}\tilde{Z}}|}{10^{-7}} \right)^{-2} \left(\frac{m_{\tilde{a}}}{5 \text{ keV}} \right)^{-3} \left(\frac{f_a}{10^{11} \text{ GeV}} \right)^2. \quad (4)$$

In a similar manner, gravitino can also live long enough to be considered as dark matter though it is governed by a different set of couplings. In a recent analysis by Buchmueller et. al [13] it has been shown that gravitinos of mass $\mathcal{O}(5 \text{ GeV})$ or just above are compatible with thermal leptogenesis, cold dark matter and Big Bang Nucleosynthesis. However, purely from a dark matter relic density point of view, it has been shown by Rubakov et. al [14] that a lighter gravitino of the order of a keV could as well be consistent with relic density observations as a warm dark matter candidate. In the presence of bilinear R-parity violation, gravitino decays into a neutrino and a photon [13, 15]. The decay rate is given by the expression [16] :

$$\Gamma(\psi_{3/2} \rightarrow \gamma \nu) = \frac{1}{32\pi} |U_{\tilde{\gamma}\nu}|^2 \frac{m_{3/2}^3}{M_P^2}, \quad (5)$$

where $m_{3/2}$ is the gravitino mass and M_P is the Planck scale, and $U_{\tilde{\gamma}\nu}$ is given by [13]

$$U_{\tilde{\gamma}\nu} \simeq g_z \left| \sum_{\alpha=1}^4 c_{\tilde{\gamma}\nu} c_{\tilde{z}\alpha}^* \frac{v_\nu}{m_{\chi_\alpha^0}} \right| \sim 10^{-8} \left(\frac{\epsilon_3}{10^{-7}} \right) \left(\frac{\tilde{m}}{200 \text{ GeV}} \right)^{-1} \sim 10^{-5} \left(\frac{\epsilon_3}{10^{-4}} \right) \left(\frac{\tilde{m}}{200 \text{ GeV}} \right)^{-1}, \quad (6)$$

Here, g_z is the gauge coupling, $c_{\tilde{\gamma}\nu}$ and $c_{\tilde{z}\alpha}$ are the mixing elements in the neutralino-neutrino mixing matrix, v_ν is the sneutrino VEV, \tilde{m} is a common mass scale for the superpartners and ϵ_3 is the bilinear R-parity violating parameter defined in Eq.(1). These parameters appearing in the second term of the RHS can be found in [13]. Using this formula for the lifetime of a 5 keV gravitino we find ,

$$\tau_{3/2}^{2\text{-body}} \simeq 3 \times 10^{40} s \left(\frac{\epsilon_3}{10^{-4}} \right)^{-2} \left(\frac{\tilde{m}}{200 \text{ GeV}} \right)^2 \left(\frac{m_{3/2}}{5 \text{ keV}} \right)^{-3}. \quad (7)$$

From the above we see that the lifetime of the gravitino is several orders larger compared to the age of the universe ($\mathcal{O}(10^{18} \text{ s})$).

Since, according to the above expressions, their lifetimes are large but finite, one would expect a few of the axinos/gravitinos to decay through the two body processes (2) and (5). The resultant photons are in the X-ray regime and thus could be observed by the astrophysical X-ray telescopes. These X-rays would constitute an excess over the astrophysical background. In the recent years, there has been a report of such an observation by the Chandra satellite based observatory with a line emission at $2.5 \pm 0.11 \text{ keV}$ (90% CL) and flux of $(3.53 \pm 2.77) \times 10^{-6} \text{ photons cm}^{-2} \text{ s}^{-1}$ at (90% CL) [17].

Recently, Loewenstein and Kusenko [18] have tried to explain the Chandra excess [17] through a radiative decay of a sterile neutrino of mass of 5 keV. It should be noted that astrophysical X-rays have been observed earlier too from the Suzaku satellite and have led to stringent constraints on sterile neutrino mixing and mass parameters [19]. In the present work, we would like to obtain similar constraints on the axino masses and the Peccei-Quinn symmetry breaking scale f_a for a fixed value of the neutralino-neutrino mixing parameter satisfying neutrino data, using the Chandra results. On the other hand, similar analysis on gravitino dark matter does not provide any constraint because of the larger suppression through $1/M_{P_l}^2$ in the decay width.

II. DARK MATTER HALOS AND FLUX OF X-RAY PHOTONS

The X-ray flux from the dark matter halos can be calculated for a given galaxy knowing its luminosity distance and the dark matter distribution. In the following we outline the calculation of the flux in general and apply it for our own galaxy.

An object such as a field galaxy or dwarf galaxy or a cluster of galaxies possessing a dark matter halo of mass M_{DM} will be composed of $N = M_{DM}/m_X$ dark matter particles of rest mass m_X . If Γ_X is the dark matter particle decay rate into photons of energy E_γ , then the total associated X-ray luminosity is [20]

$$\mathcal{L} = \frac{E_\gamma}{m_X} M_{DM} \Gamma_X. \quad (8)$$

Here we have assumed that the halo is relatively nearby and that redshift effects on the luminosity are negligible.

We will also consider the simple case where $E_\gamma = m_X/2$ (when the neutrino mass is negligible compared to that of the dark matter candidate), which is relevant for the two body decays which are the focus of the present work. The flux from an object seen through the telescope is simply

$$F = \frac{\mathcal{L}}{4\pi D_L^2}, \quad (9)$$

where D_L is the luminosity distance to the object. This can be taken to be the coordinate distance r from the earth to the dark matter site (neglecting redshift effect).

With $E_\gamma = m_X/2$ we get

$$\mathcal{L} = \frac{M_{DM} \Gamma_X}{2}. \quad (10)$$

Hence, the flux F can be written as

$$\begin{aligned} F &\approx \frac{\Gamma_X}{2} \int_{l.o.s} \frac{1}{4\pi r^2} dM_{DM} \\ &= \frac{\Gamma_X}{8\pi} \int_{l.o.s} \frac{1}{r^2} \rho_{DM}(r) r^2 dr d\Omega, \end{aligned} \quad (11)$$

where $\rho_{DM}(r)$ is the density of dark matter particle as a function of distance from the galactic centre. In order to calculate the flux which is coming from the direction of the galactic anti-center, we have

$$F = \frac{\Gamma_X \Omega}{8\pi} \int_{r_\odot}^{\infty} \rho_{DM}(r) dr. \quad (12)$$

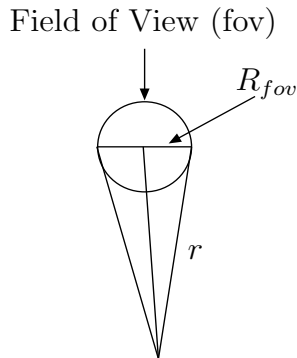


FIG. 1: Solid angle (Ω) calculation of the dark matter halo.

The flux which is coming from the direction of the galactic center is given by

$$F = \frac{\Gamma_X \Omega}{8\pi} \int_{-\infty}^{r_\odot} \rho_{DM}(r) dr. \quad (13)$$

Here r_\odot ($\simeq 8$ kpc) is the distance of an observer on the earth from the galactic centre (of Milky Way). Note that this derivation applies to integration along the Milky Way only. The reason we are considering Milky Way is because of the fact that it is a very extended source of the dark matter halo and SPI telescope (which has a wide field of view) is well suited for such an extended object. Our analysis on SPI telescope will be presented in Sec. IV and we shall show that this will give a very strong constraint on the axino dark matter model.

In order to determine the dark matter halo contribution to the X-ray flux, one needs to know the distribution of the DM in the halo of the Milky Way. In Eq.(11), Ω is the small ($\ll 1$) solid angle corresponding to the field of view of the telescope which can be calculated from figure 1. In figure 1, the projected radius of the field of view is denoted by R_{fov} , and the angular field of view by θ . Approximating Ω as the solid angle of a cone with an apex angle θ , we have

$$\Omega = \frac{\pi\theta^2}{4}, \quad (14)$$

where

$$\theta = \frac{2R_{fov}}{r}. \quad (15)$$

In particular for ACIS aboard Chandra, $\theta \approx 5 \times 10^{-3}$ rad, which determines the solid angle. Later on we shall show that a much larger solid angle is obtained for SPI.

The final input needed in the calculation of the flux is $\rho_{DM}(r)$, the density profile of the dark matter. While the actual profile of the dark matter in the galaxy is unknown, there are

many profiles put forward in the literature. Many of them also have analytical expressions. For example, the isothermal profile [21] is given by

$$\rho_{\text{DM}}(r) = \frac{v_h^2}{4\pi G_N} \frac{1}{r_c^2 + r^2}, \quad (16)$$

where v_h corresponds to the contribution of the DM halo into the galactic rotation curve in its flat part, $v_h \approx 170$ km/s. Here the core radius r_c is almost 4 kpc. Now, the profile integral in Eq.(12) for the galactic anti-centre is

$$\int_{r_\odot}^{\infty} \rho_{\text{DM}}(r) dr = \frac{C}{r_c} \left[\frac{\pi}{2} - \tan^{-1} \left(\frac{r_\odot}{r_c} \right) \right] = \frac{C}{r_c} \tan^{-1} \left(\frac{r_c}{r_\odot} \right), \quad (17)$$

where $C = v_h^2/4\pi G_N$. Similarly for the galactic centre case from Eq.(13):

$$\int_{-\infty}^{r_\odot} \rho_{\text{DM}}(r) dr = \frac{C}{r_c} \left[\frac{\pi}{2} + \tan^{-1} \left(\frac{r_\odot}{r_c} \right) \right]. \quad (18)$$

Using Eqs.(17) and (18) one can calculate the flux from the galactic anti-center and galactic center, respectively.

Once again let us mention that the calculation of the dark matter line flux in the direction of the Galactic center or anti-center has been performed just for simplicity. In general one can calculate the flux coming from any given direction on the sky. We shall present our analysis for an angular distance 13° between the given direction on the sky and the direction towards the Galactic center when we present our results for SPI.

Another point is that in Eq.(12) and (13) the upper (lower) limit of integration is actually not infinite but depends on the assumed size of the Milky Way dark matter halo. However, since the integral is converging, we shall obtain the same result as long as the limit is 200 kpc or above. This is the reason we have assumed the upper (lower) limit to be infinite just for simplicity.

The data from Virgo cluster by ACIS aboard Chandra has been analyzed in Ref. [20]. The instrumental background has been estimated to be 2×10^{-2} cts s^{-1} in a 200 eV energy bin. It has been shown that in order to detect a dark matter decay line signal of energy $E_\gamma = m_X/2$ at 4σ level, one must observe a flux above the value, $F_{\text{det}} = 10^{-13}$ erg $\text{cm}^{-2}\text{sec}^{-1}$ with an integration time of 36 ksec for observation. In our analysis of the Milky Way dark matter halo, we shall assume that the same flux limit is applicable in the entire x-ray energy range of 1 keV to 8 keV relevant for Chandra telescope. This determines the region of the parameter space for any theoretical scenario, which can be probed by Chandra.

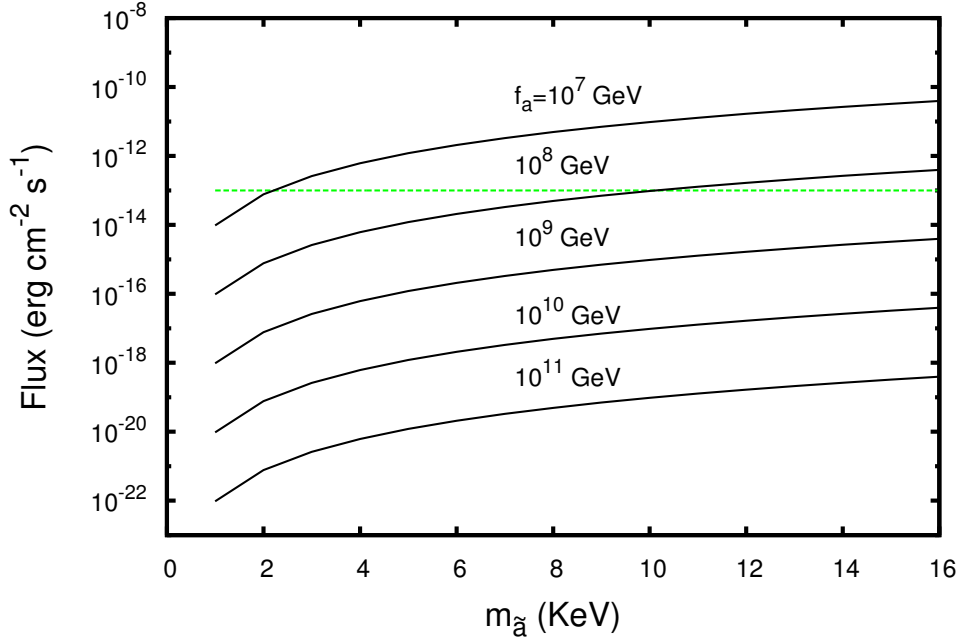


FIG. 2: Flux of photons from the Milky Way galactic centre for the Max. disk model A_2 . The horizontal line is the lower limit of detectability of the flux applicable for the Chandra X-ray satellite observations as explained in the text.

III. NUMERICAL ANALYSIS FOR CHANDRA TELESCOPE

We have taken the value of the neutrino-neutralino mixing parameter ($\xi_i U_{\tilde{\gamma}\tilde{Z}} \equiv U_{\tilde{\gamma}\nu}$) to be 9×10^{-7} , which is the allowed value from neutrino data. In figure 2, we show the flux from the Milky Way galactic centre as a function of the axino mass $m_{\tilde{a}}$, following the Max. disk model A_2 [22] of NFW profile [23, 24] for various values of f_a . As can be seen from the figure, the lower is the values of f_a , the larger is the flux. From the figure we see that for the astrophysically unconstrained range of the Peccei-Quinn symmetry breaking scale, namely, $f_a \gtrsim 10^9$ GeV [25], the axino mass is unrestricted in the range shown in the figure. However, for lower values of f_a some constraint can be obtained.

The question that arises is: for which profiles there exist constraints from Chandra within the astrophysically unconstrained values of f_a . In figure 3 we present the fluxes for various profiles including the isothermal profile discussed in the previous section. The isothermal [21], and the NFW profiles [22, 26] do not provide constraint if one takes the lower limit on

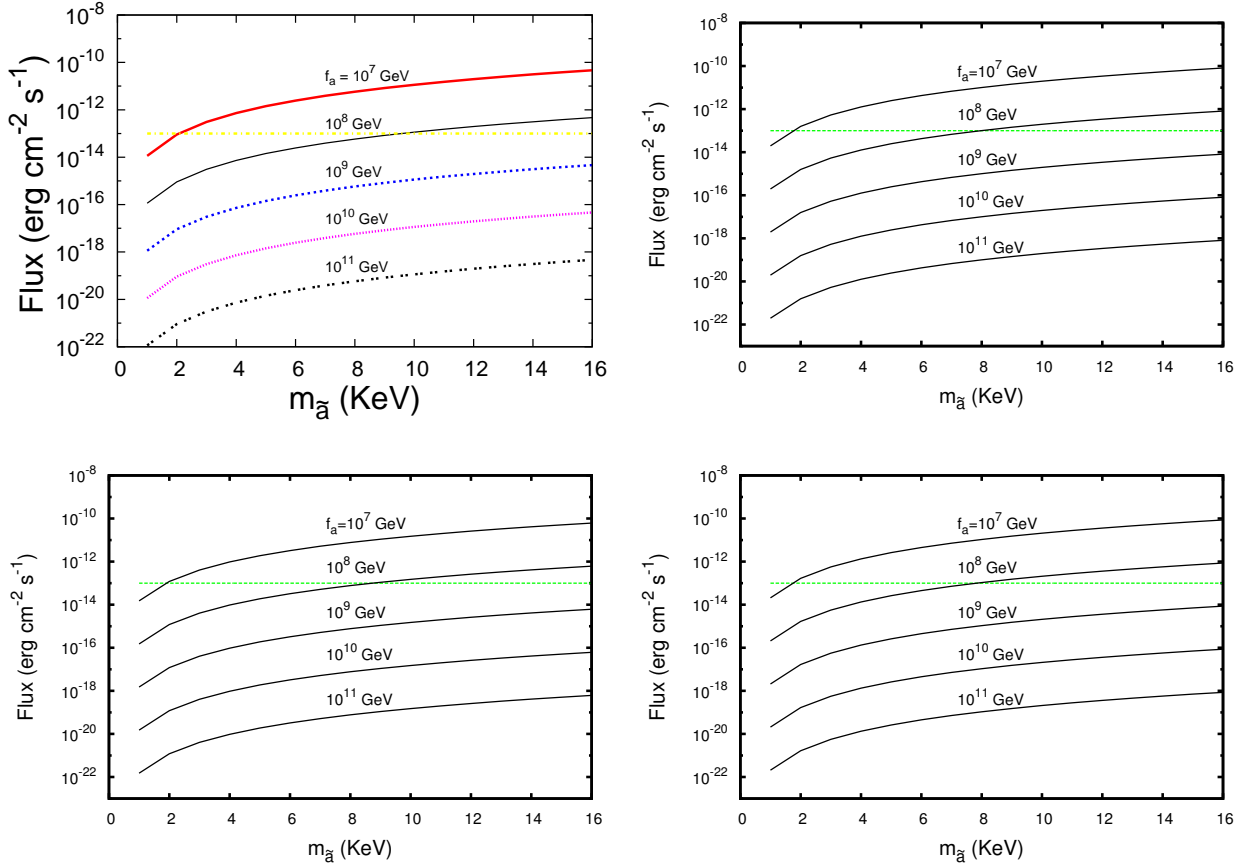


FIG. 3: Flux of photons from the Milky Way galactic centre for various profiles. Top left is for isothermal profile, top right is for the NFW favored models (A_1 or B_1) [22]. Similarly, bottom left is for the NFW Max. disk models B_2 of the MW DM halo whereas bottom right is for the NFW profile best fit parameters given by Battaglia et al [26]. As before the horizontal line is the lower limit of the flux applicable for the Chandra X-ray satellite observations.

$f_a \gtrsim 10^9$ GeV strictly. However, there are ways of avoiding these astrophysical constraints in some situations such as (a) existence of paraphotons [27, 28] and (b) existence of temperature dependent couplings [29]. In either case, f_a lower limit can be relaxed, sometimes even to values of $\mathcal{O}(10^6)$ GeV. In such situations the constraints from Chandra could play an important role.

Before concluding let us briefly touch the constraints on our model coming from the observation of the Virgo clusters [20, 30, 31]. Using Eqs.(4), (9) and (10), the flux from a

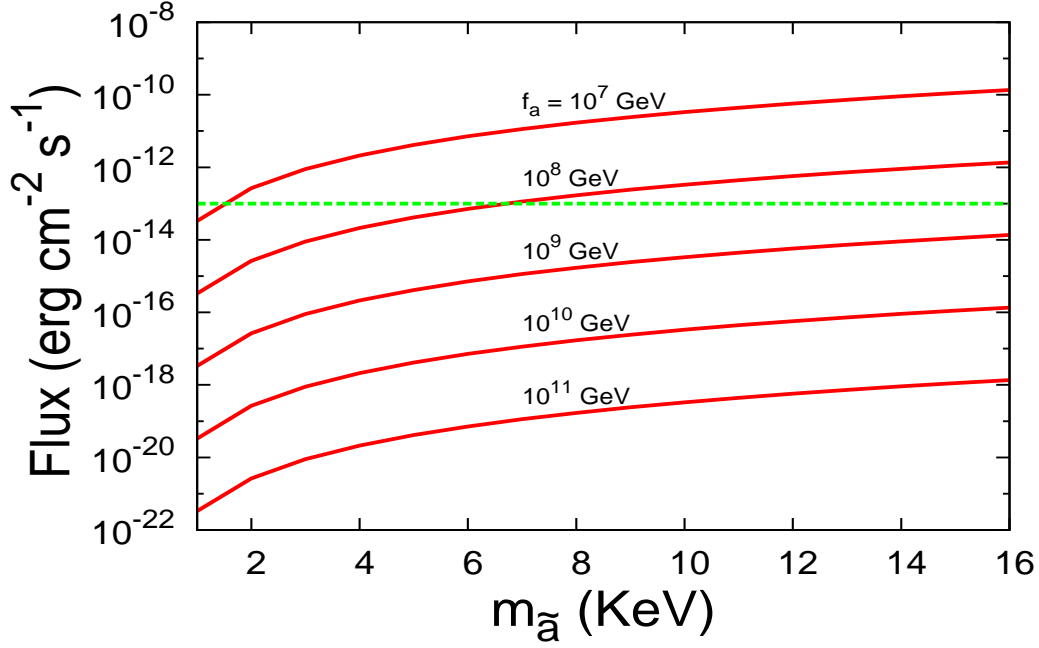


FIG. 4: Flux of photons from the centre of the Virgo cluster. As before the horizontal line is the lower limit of the flux applicable from the Chandra X-ray satellite observations.

cluster can be written as,

$$F \approx 2.19 \times 10^{-21} \text{ ergs cm}^{-2} \text{ s}^{-1} \left(\frac{D_L}{1 \text{ Mpc}} \right)^{-2} \left(\frac{M_{\text{DM}}^{\text{fov}}}{10^{11} M_{\odot}} \right) \left(\frac{U_{\tilde{\gamma}\nu}}{10^{-7}} \right)^2 \left(\frac{m_{\tilde{a}}}{5 \text{ keV}} \right)^3 \left(\frac{f_a}{10^{11}} \right)^{-2} \quad (19)$$

The values for D_L and $M_{\text{DM}}^{\text{fov}}$ for the Virgo cluster are given in [20]. We have used $M_{\text{DM}}^{\text{fov}} = 10^{13} M_{\odot}$ and $D_L = 20.7 \text{ Mpc}$ in Eq.(19) and demanded that the flux should be less than the detectable limit $10^{-13} \text{ ergs cm}^{-2} \text{ s}^{-1}$. The results are plotted in figure 4. It is evident that the constraints obtained, are at least as stringent as those for the Milky Way, for the more optimistic density profiles. Since the luminosity distance D_L is much larger for the Virgo cluster, one would expect that the corresponding flux will be smaller than that obtained for Milky Way. For the Virgo cluster, however, the total dark matter mass in the field of view ($M_{\text{DM}}^{\text{fov}}$) is much larger compared to that of the Milky Way in a particular direction (say, the direction of the galactic center or anti-center). This large mass for Virgo cluster compensates for the large luminosity distance and hence the resulting flux becomes comparable to the flux from Milky Way for more optimistic density profiles such as the NFW favored model A_1 or B_1 [22].

IV. NUMERICAL ANALYSIS FOR SPI

In this section we shall look at the bounds on the axino parameters originating from an analysis based on the data from the high-resolution spectrometer SPI on board the INTEGRAL satellite [32]. SPI is sensitive to X-ray photons in the energy range 20 keV to 7 MeV. Obviously, the data from SPI is applicable to axinos in the mass range of 40 keV to 14 MeV. However, we shall restrict ourselves to the axino mass range of 40 keV to 400 keV, which includes the window on the axino mass where the axino can act as a warm dark matter candidate. The negative search of a dark matter decay line using SPI put restrictions on the dark matter decay line flux [32]. Using this flux restrictions we derive bound on the axino mass parameters.

In our simple minded analysis, we have used the *partially coded field of view* of the SPI detector given by $\theta_{PCFOV} \approx 35^\circ$. This corresponds to a solid angle $\Omega = 2\pi(1 - \cos(\theta_{PCFOV}/2)) \approx 0.29$ and we have used this value of the solid angle for our numerical calculation. The dark matter decay line flux has been calculated using various profiles mentioned in the previous section. In addition, we have used the *minimal model* described in Ref.[32], for which the dark matter density is constant within r_\odot whereas it is given by the model A_2 of Klypin et al in Ref. [22] for $r > r_\odot$.

The results obtained in Ref.[32] using the SPI data set is applicable to any model of decaying dark matter. We have used the results shown in figure 11 of Ref.[32], for the 3σ restrictions on the lifetime of the dark matter particle as a function of the X-ray photon energy ¹. Using the *minimal model* for the dark matter profile as mentioned above, we translate this restriction on the lifetime into a restriction on the decay line flux as a function of the axino mass. The dark matter decay line flux is also a function of the angular distance ϕ between the direction along the line of sight and the direction towards the Galactic center. We have used $\phi = 13^\circ$ (the inner Galaxy) for the calculation of the flux restriction.

In figure 5 we show the flux restriction using the red zigzag curve. In addition, in the same figure we show the line flux as a function of the axino mass coming from an axino dark matter, for different values of f_a . These curves are drawn for the minimal profile of [32].

From the figure we see that for the astrophysically unconstrained range of the Peccei-

¹ We sincerely thank Oleg Ruchayskiy for providing us with the data file corresponding to figure 11 of their paper.

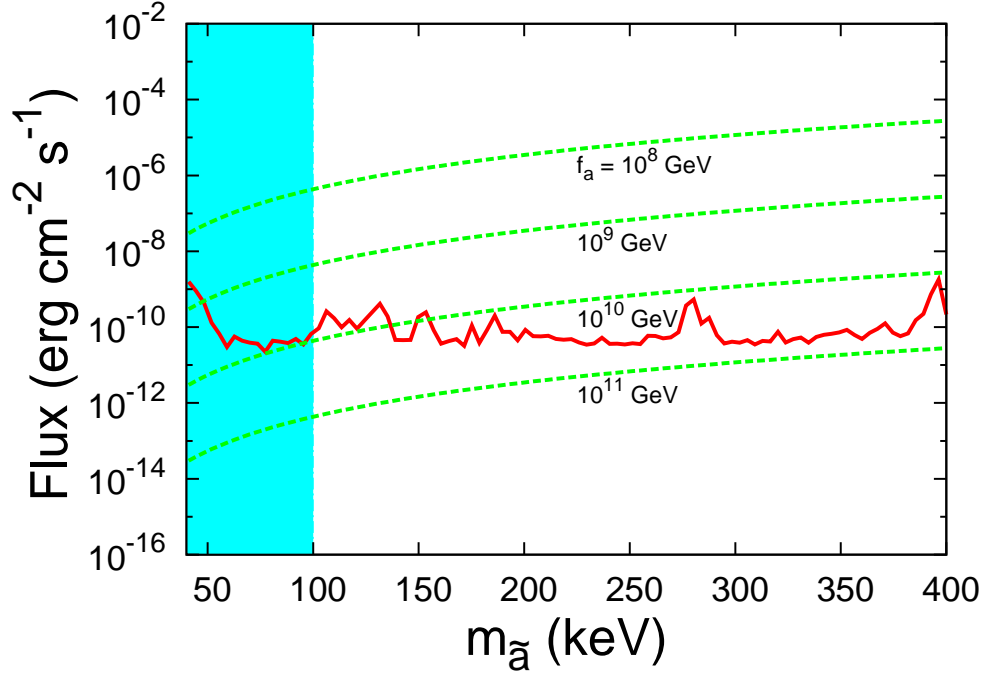


FIG. 5: Flux of photons from the Milky Way inner Galaxy ($\phi = 13^\circ$) for the minimal profile described in the text. The red zigzag line is the lower limit of the flux coming from the negative search of a dark matter decay line using the data from SPI spectrometer on board the INTEGRAL satellite. The shaded region is the window on the axino mass where the axino can act as a warm dark matter candidate.

Quinn symmetry breaking scale, namely, $f_a \gtrsim 10^9$ GeV [25], axino mass $m_{\tilde{a}} \gtrsim 50$ keV could be excluded by SPI data.

On the other hand, the results depend on the profile one chooses for the dark matter in the Milky Way. In particular, this dependence is more pronounced in the direction of the inner Galaxy. In figure 6 we plot the flux for a fixed value of f_a for the isothermal profile and different models of the NFW profile (the values of the different parameters appearing in these profiles are taken from [32]) as well as the minimal profile of [32]. The shaded region and the zigzag line have the same meaning as before. From the figure it is obvious that there could be some noticeable variation in the flux depending on the profile one uses. Accordingly this gives us different upper bounds on the axino mass parameter. However, this variation becomes more and more negligible for some of the profiles if one looks at the direction of the Galactic anti-center.

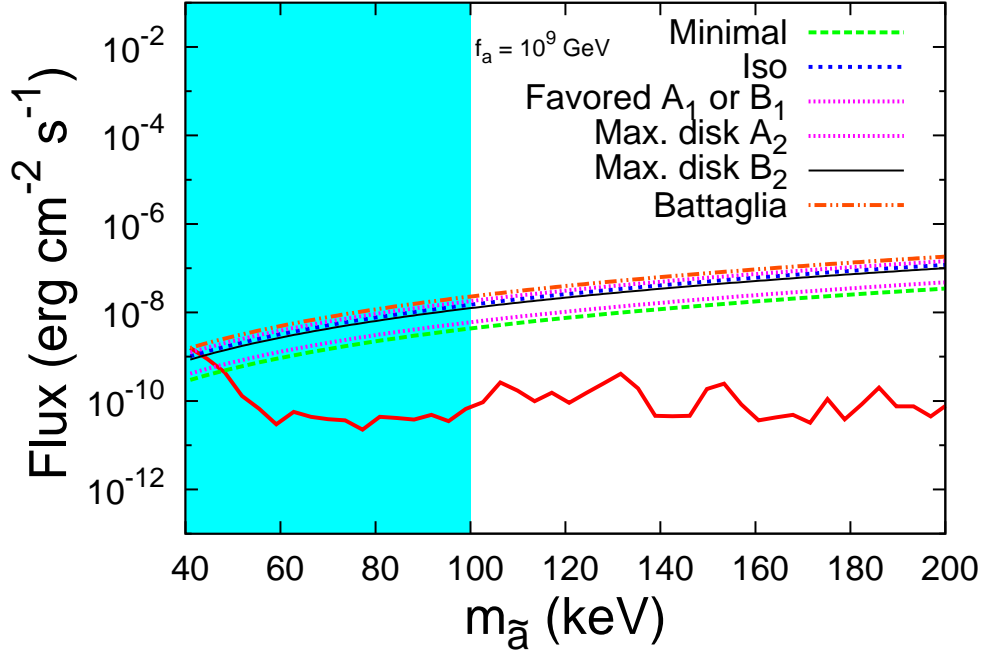


FIG. 6: Flux of photons from the Milky Way inner Galaxy ($\phi = 13^\circ$) for all profiles for $f_a = 10^9$ GeV. As before, the red zigzag line is the lower limit of the flux coming from the SPI spectrometer observations. The shaded region is the window on the axino mass where the axino can act as an warm dark matter candidate.

V. SUMMARY, CONCLUSIONS AND OUTLOOK

We have attempted to constrain the parameter space of a warm dark matter candidate from the non-observation of galactic X-ray line flux at the X-ray telescopes such as Chandra and SPI. We are considering an R-parity violating SUSY scenario, where the gravitino and the axino are the two likely candidates of warm dark matter. Due to the violation of lepton number, they can have *some* two body decays into a (monochromatic) photon and a neutrino, although their mean lifetimes are larger than the age of the universe. These photons correspond to X-ray lines that are potentially observable at X-ray telescopes.

We have found that gravitino decays in the above channel yield too small a flux to lead to any useful constraint, due to the suppression of gravitino interaction by the Planck mass. The axino, on the other hand, couples with a strength inversely proportional to the Peccei-Quinn symmetry breaking scale (f_a), which can lie in the range 10^9 – 10^{12} GeV, and is therefore

more promising from the viewpoint of X-ray satellite observations. Our analysis is based on the assumption that R-parity violation, triggered by bilinear terms in the superpotential, is of such a degree as to accommodate the pattern of neutrino masses and mixing suggested by the solar and atmospheric neutrino data. On this basis, we find that the limits from Chandra and SPI disallow a sizable part of the yet allowed axino parameter space defined by the axino mass ($m_{\tilde{a}}$) and f_a . In particular, axino masses in the range $\sim 50 - 100$ keV tend to be disallowed by SPI. The best results follow from a study of X-rays from the inner part of the Milky Way. For galaxy clusters such as the Virgo cluster a similar analysis has been performed for Chandra with similar conclusions as in the case of Milky Way.

If one uses the exact expressions for neutrino masses, there could be some SUSY parameter space dependence of the above results. In particular, there could be some cancellations in the expression for sneutrino VEV in some regions of the parameter space. However, the general conclusions, based on the limits on the extent of R-parity violation, are unlikely to differ drastically from what have been derived above.

It should be noted that the limits have some dependence on the profile of the dark matter. The flux from the inner part of the galaxy can vary significantly depending on the profile. For some profiles like NFW favored models A_1 or B_1 , NFW parameters of Battaglia et al, there could be constraints for $f_a = 10^9$ GeV and $m_{\tilde{a}} \gtrsim 42$ keV. Even constraints can be obtained for $f_a = 10^{10}$ GeV from SPI data. On the whole, for the lower range of allowed f_a , namely, 10^{9-10} GeV, axino masses above 42-60 keV (depending on f_a) can be ruled out from the SPI data on Milky Way.

At the end, we would like to remark that the Chandra observatory is a high resolution experiment, but its energy range for X-rays is restricted to 8 keV. Similarly, for SPI the energy range is 20 keV to 7 MeV. There are other experiments; among them, XMM-Newton has less resolution but energy range up to 12 keV [33]. Beppo-SAXX can detect X-rays up to 15 keV [34]. Old experiments like HEAO-I, and HEAO-III can measure X-rays up to 10 MeV. HEAO-II (Einstein) can measure X-rays up to 20 keV [35]. Japan's fifth X-ray satellite Suzaku can carry out high resolution spectroscopic observations in a wide energy range of 0.3 keV to 600 keV [36]. A global analysis based on all of these experiments can lead to further insight into decaying warm dark matter candidates in an R-parity violating scenario.

Acknowledgments

We thank Oleg Ruchayskiy for many helpful discussions. The work of BM was partially supported by funding available from the Department of Atomic Energy, Government of India, for the Regional Centre for Accelerator-based Particle Physics (RECAPP), Harish-Chandra Research Institute. SKV acknowledges support from DST project “Complementarity between direct and indirect searches for Supersymmetry”. PD is supported through the Gottfried Wilhelm Leibniz Program by the Deutsche Forschungsgemeinschaft (DFG). PD, BM and SR thank Centre for High Energy Physics, Indian Institute of Science, Bangalore, for hospitality during the initial stages of this work. SKV and BM acknowledge the hospitality of the Department of Theoretical Physics, Indian Association for the Cultivation of Science, Kolkata, while this work was on. SR and SKV also thank RECAPP for hospitality during the final stages of this work. SR thanks the CERN Theory group for hospitality during the preparation of the revised version of the work.

-
- [1] J.E. Kim, A. Masiero and D.V. Nanopoulos, Phys. Lett. **B139**, 346 (1984).
 - [2] E.J. Chun, J.E. Kim and H.P. Nilles, Phys. Lett. **B287**, 123 (1992).
 - [3] E.J. Chun and A. Lukas, Phys. Lett. **B357**, 43 (1995).
 - [4] J.M. Frere and J.M. Gerard, Lett. Nuovo Cim. **37**, 135 (1983).
 - [5] H.B. Kim and J.E. Kim, Phys. Lett. **B527**, 18 (2002).
 - [6] D. Hooper and L. T. Wang, Phys. Rev. **D70**, 063506 (2004); E.J. Chun and H.B. Kim, J. High Energy Phys. **10**, 082 (2006).
 - [7] L. Covi, H.B. Kim, J.E. Kim and L. Roszkowski, JHEP **05**, 033 (2001); L. Covi and J.E. Kim, arXiv:0902.0769.
 - [8] O. Seto and M. Yamaguchi, Phys. Rev. **D75**, 123506 (2007).
 - [9] J.L. Feng, M. Kamionkowski and S.L. Lee, Phys. Rev. **D82**, 015012 (2010).
 - [10] S. Biswas, J. Chakraborty and S. Roy, Phys. Rev. **D83**, 075009 (2011).
 - [11] L.J. Hall and M. Suzuki, Nucl. Phys. **B231**, 419 (1984); F. de Campos, M.A. Garcia-Jareno, A. S. Joshipura, J. Rosiek and J.W.F. Valle, Nucl. Phys. **B451**, 3 (1995); A.S. Joshipura and M. Nowakowski, Phys. Rev. **D51**, 2421 (1995); R. Hempfling, Nucl. Phys. **B478**, 3 (1996);

- S. Roy and B. Mukhopadhyaya, Phys. Rev. **D55**, 7020 (1997); M.A. Diaz, J.C. Romao and J.W.F. Valle, Nucl. Phys. **B524**, 23 (1998); B. Mukhopadhyaya, S.Roy and F. Vissani, Phys. Lett. **B443**, 191 (1998); A.S. Joshipura and S.K. Vempati, Phys. Rev. **D60**, 095009 (1999); E.J. Chun, S.K. Kang, C.W. Kim and U.W. Lee, Nucl. Phys. **B544**, 89 (1999); A. Datta, B. Mukhopadhyaya, and S. Roy, Phys. Rev. **D61**, 055006 (2000); A.S. Joshipura, R.D. Vaidya and S.K. Vempati, Phys. Rev. **D65**, 053018 (2002); M. Hirsch, W. Porod, J.C. Romao and J.W.F. Valle, Phys. Rev. **D66**, 095006 (2002); M.A. Diaz, M. Hirsch, W. Porod, J.C. Romao and J.W.F. Valle, Phys. Rev. **D68**, 013009 (2003), Erratum-ibid. **D71**, 059904 (2005).
- [12] J.E. Kim, Phys. Rev. **D58**, 055006 (1998).
- [13] W. Buchmuller, L. Covi, K. Hamaguchi, A. Ibarra, T. Yanagida, J. High Energy Phys. **03**, 037 (2007).
- [14] D. Gorbunov, A. Khmelnitsky, V. Rubakov, J. High Energy Phys. **12**, 055 (2008).
- [15] F. Takayama and M. Yamaguchi, Phys. Lett. **B476**, 116 (2000).
- [16] F. Takayama and M. Yamaguchi, Phys. Lett. **B485**, 388 (2000).
- [17] See, the NASA website http://www.nasa.gov/mission_pages/chandra/main/index.html
- [18] M. Loewenstein and A. Kusenko, Astrophys. J. **714**, 652 (2010).
- [19] M. Loewenstein and A. Kusenko, Astrophys. J. **700**, 426 (2009).
- [20] K. Abazajian, G.M. Fuller and W.H. Tucker, Astrophys. J. **562**, 593 (2001).
- [21] A. Boyarsky, A. Neronov, O. Ruchayskiy, M. Shaposhnikov and I. Tkachev, Phys. Rev. Lett. **97**, 261302 (2006).
- [22] A. Klypin, H. Zhao, R.S. Somerville, ApJ **573**, 597 (2002) (astro-ph/0110390).
- [23] J.F. Navarro, C.S. Frenk and S.D.M. White, Astrophys. J. **490** 493 (1997).
- [24] A. Boyarsky, J. Nevalainen and O. Ruchayskiy, Astron. Astrophys. **471**, 51 (2007).
- [25] For a recent summary of astrophysical and other constraints on f_a , see, for example, F.D. Steffen, Eur. Phys. J. C **59**, 557 (2009) and references therein.
- [26] G. Battaglia *et al.*, Mon. Not. Roy. Astron. Soc. **364**, 433 (2005) (astro-ph/0506102).
- [27] E. Masso and J. Redondo, J. Cosmology and Astroparticle Phys., **09**, 015 (2005).
- [28] E. Masso and J. Redondo, Phys. Rev. Lett. **97**, 151802 (2006).
- [29] J. Jaeckel, E. Masso, J. Redondo, A. Ringwald and F. Takahashi, Phys. Rev. **D75**, 013004 (2007).
- [30] A. Boyarsky, A. Neronov, O. Ruchayskiy and M. Shaposhnikov, Phys. Rev. **D74**, 103506

(2006).

- [31] For a recent analysis, see, R.S. Hundi and S. Roy, arXiv:1105.0291.
- [32] A. Boyarsky, D. Malyshev, A. Neronov, and O. Ruchayskiy, arXiv:0710.4922.
- [33] See, the NASA website <http://heasarc.nasa.gov/docs/xmm/xmm.html>.
- [34] See, the official website, <http://www.asdc.asi.it/bepposax/>
- [35] See, the NASA website <http://heasarc.nasa.gov/docs/einstein/heao2.html>.
- [36] See, the suzaku website <http://www.darts.isas.jaxa.jp/astro/suzaku/>

